

DLoRA: Distributed Parameter-Efficient Fine-Tuning Solution for Large Language Model

Chao Gao^{*1} and Sai Qian Zhang^{†2}

¹University of California, Riverside

²New York University

Abstract

To enhance the performance of large language models (LLM) on downstream tasks, one solution is to fine-tune certain LLM parameters and make it better align with the characteristics of the training dataset. This process is commonly known as parameter-efficient fine-tuning (PEFT). Due to the scale of LLM, PEFT operations are usually executed in the public environment (e.g., cloud server). This necessitates the sharing of sensitive user data across public environments, thereby raising potential privacy concerns. To tackle these challenges, we propose a distributed PEFT framework called *DLoRA*. *DLoRA* enables scalable PEFT operations to be performed collaboratively between the cloud and user devices. Coupled with the proposed Kill and Revive algorithm, the evaluation results demonstrate that *DLoRA* can significantly reduce the computation and communication workload over the user devices while achieving superior accuracy and privacy protection.

1 Introduction

Large Language Models (LLMs) have recently incited substantial public interest. Their ability to grasp context and nuance enables them to handle natural language processing (NLP) tasks such as text generation (Brown et al., 2020; Zhuang et al., 2023), translation (Zhu et al., 2023; Hadi et al., 2023) and summarization (Zhang et al., 2023b) with remarkable proficiency. Because of the extensive number of parameters in LLMs and the substantial computational workload during their operations, LLMs are usually implemented on nodes with rich compute resources such as cloud servers (OpenAI and Microsoft; Badr, 2023). During operation, users send their data to the cloud server for LLM processing, after which the LLM results are transmitted back to the user devices.

Previous studies (Brown et al., 2020) has shown that LLMs can extend their learned knowledge to novel tasks not seen during the training phase, a phenomenon commonly referred to as *zero-shot* capability. However, fine-tuning still remains essential to enhance LLM performance on unseen user datasets and tasks. Due to its scale, a widely adopted strategy for fine-tuning LLMs involves adjusting a limited number of LLM parameters while keeping the remainder unchanged. This approach, termed *parameter-efficient-fine-tuning* (*PEFT*), adds small modules of parameters to pre-defined positions of the pre-trained LLM and only fine-tunes these modules (Houlsby et al., 2019; Guo et al., 2020a; Mao et al., 2021a; Karimi Mahabadi et al., 2021a) over the downstream tasks to better adapt to the user data.

While PEFT presents an efficient approach for improving LLM performance, it also poses significant challenges for system deployment. To deploy PEFT, one potential solution involves transferring user input to the cloud, and the entire PEFT process is performed over the cloud servers. This scheme is referred to as *Cloud-only* solution (Figure 1 (a)). However, this approach comes with several drawbacks. On one hand, keeping private user data in a shared cloud environment raises immediate privacy concerns. On the other hand, in order to deliver a personalized LLM service, it is necessary to create and fine-tune a separate set of personal LLM parameters using the training dataset from each user. This can result in significant scalability challenges as the user group expands in size. By contrast, another option is to offload the LLM fine-tuning process completely to the user device, presented as *Edge-only* solution in Figure 1 (b). Unfortunately, this approach is often impractical due to the limited computational resources available on user devices.

To mitigate the aforementioned system problems, in this work we propose a distributed PEFT solu-

*Email: cgao037@ucr.edu

†Email: sai.zhang@nyu.edu

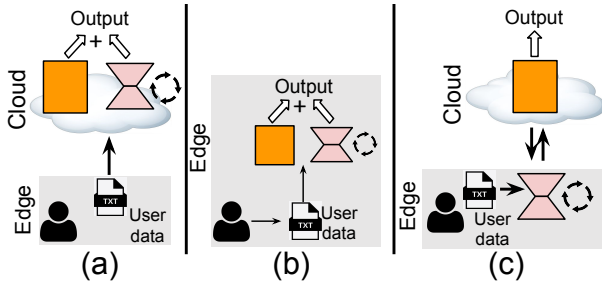


Figure 1: (a) Cloud-only solution. (b) Edge-only solution. (c) DLoRA scheme. The frozen and learnable parameters are shown in orange and red, respectively.

tion named *DLoRA* (Figure 1 (c)) for collaborative PEFT operations between a cloud server and user device. *DLoRA* eliminates the need to deliver private user data for LLM fine-tuning in the cloud thereby ensuring the personal LLM parameters are stored completely within the user device, thereby minimizing the risk of privacy leakage. Additionally, *DLoRA* offloads partial computational workload for LLM fine-tuning to user devices, effectively mitigating the scalability issues.

Beyond that, our preliminary studies on conventional PEFT algorithms suggests that the majority of trainable parameters within LLM remain fairly constant throughout the fine-tuning process, with only a small subset of parameters undergoing active changes. This group of changing parameters varies with the training dataset and downstream tasks. Motivated by this observation, we introduced a *Kill and Revive (KR)* algorithm for *DLoRA* that dynamically identifies and fine-tunes the set of LLM parameters most responsive to the training data, resulting in a substantial reduction in computation and communication workloads on the user devices. Overall, our contribution can be summarized as follows:

- We introduce *DLoRA*, an PEFT framework capable of executing LLM fine-tuning seamlessly between cloud and edge devices. *DLoRA* ensures the user data and personal parameters to store on user devices throughout the PEFT operation, eliminating the risk of privacy leakage while enabling scalability.
- We introduce the *Kill and Revive (KR)* algorithm for *DLoRA*, which dynamically identifies and fine-tunes the subset of LLM parameters that are most sensitive to the training data. This approach results in a notable decrease in computational and communication burdens

on user devices.

- We evaluate performed an assessment involving three LLM models across eight datasets. The evaluation results indicate that the KR algorithm can deliver an average reduction of 82% in computational load and a 87.5% reduction in communication between the user device and the cloud, while still achieving comparable or even better results than the baseline solutions.

2 Background and Related Work

In this section, we begin by introducing LLM computations in Section 2.1. We then describe the computational flow of PEFT operations in Section 2.2. After that, LLM implementation and its associated system issues in Section 2.3.

2.1 LLM Computation

To study the computations involved during the LLM execution, we explore LLaMA (Touvron et al., 2023), a popular LLM that has shown superior performance in various NLP tasks (Cui et al., 2023; Roziere et al., 2023; Zhang et al., 2023a). As illustrated in Figure 2 (a), LLaMA consists of three major components: an embedding layer, a stack of decoder blocks and a linear layer. LLaMA operate by processing text inputs from users structured as *tokens*. During the operation, an series of input tokens are first sent to the embedding layer which will convert the input tokens into numerical vectors. The outputs are then delivered to the decoder layers for further processing.

The output of the last decoder layer will be sent to a linear layer, which then generates a probability distribution spanning the complete *vocabulary* to predict the next token in the sequence. The produced token will then be concatenated with the previous tokens and used as the input for the next round of processing. This generating process repeats in an auto-regressive manner until a full sequence of tokens, referred to as a *completion*, is produced (Figure 2 (b)). For training, the computation flow is similar to that for inference, except that the generated sentences are directly compared to the ground truth output and generate the training loss. Gradients will then be computed across the LLM weights to minimize this training loss.

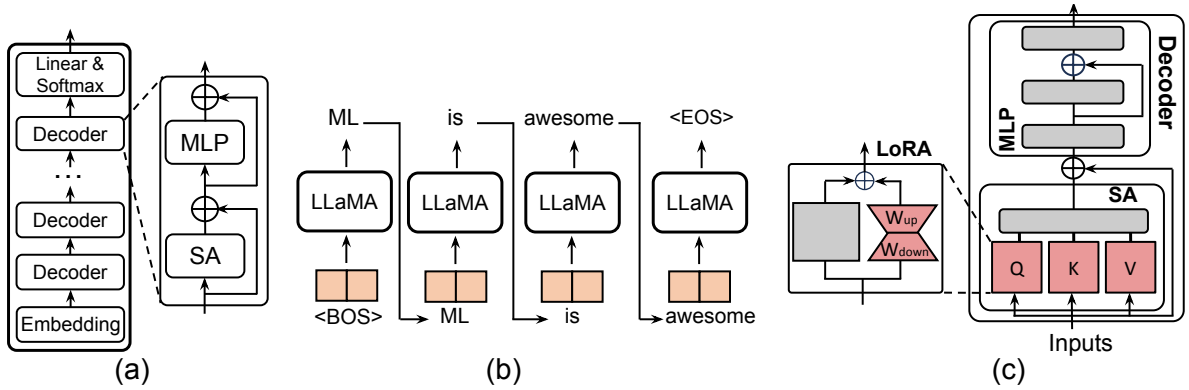


Figure 2: (a) LLaMA architecture. (b) LLaMA auto-regressive pattern. (c) LoRA operation. All the learnable components are highlighted in red, while the frozen components are highlighted in grey. LoRA is applied on all the query, key, and value blocks, we only show one of them for illustration simplicity.

2.2 Parameter Efficient Fine-Tuning

Fine-tuning is crucial for adapting LLMs to new tasks, although it also introduces several challenges, including overfitting and high computational expenses (Houlsby et al., 2019; Guo et al., 2020a; Mao et al., 2021a; Karimi Mahabadi et al., 2021a; He et al., 2021a; Zaken et al., 2021a; Valipour et al., 2022). PEFT mitigates these issues by selectively updating a subset of parameters, exemplified by LoRA (Hu et al., 2021) and Adapter techniques (Rücklé et al., 2020; Pfeiffer et al., 2020; Karimi Mahabadi et al., 2021b; Wang et al., 2022; Zhang et al., 2023d; Gao et al., 2023; He et al., 2022). LoRA introduces trainable modules within the SA blocks of LLMs, enhancing the query, key, and value generation with equations:

$$Q = (W_Q^\top + \alpha W_{up,Q}^\top W_{down,Q}) h_{in} \quad (1)$$

$$K = (W_K^\top + \alpha W_{up,K}^\top W_{down,K}) h_{in} \quad (2)$$

$$V = (W_V^\top + \alpha W_{up,V}^\top W_{down,V}) h_{in} \quad (3)$$

where W_{up} and W_{down} are LoRA’s weight matrices, h_{in} is the input, and α is a scalar hyperparameter. Adapters insert additional blocks within each decoder’s MLP block, featuring a residual connection to mitigate overfitting and computational challenges.

For clarity, we term a block of tunable LLM parameters as a *PEFT module*. For example, the PEFT module for LoRA involves all the learnable parameters within a transformer block. A collection of PEFT modules within a LLM is called *PEFT module pool*. In this work, we configure the PEFT module pool to include the LoRA parameters. However, our approach is also compatible with other PEFT schemes (e.g., Adapter).

2.3 LLM Implementation

In recent years, many cloud providers have started providing machine learning services specifically tailored to computationally intensive algorithms such as LLMs, offering APIs for seamless integration into applications. These services are vital for enhancing the computational efficiency of PEFT operations over downstream tasks (Zaken et al., 2021b; Guo et al., 2020b; Li and Liang, 2021; Wang et al., 2023; Lester et al., 2021; Mao et al., 2021b; He et al., 2021b; Liu et al., 2022; Deng, 2023; Peng et al., 2023b,a; Jeong et al., 2018; Sheng et al., 2023; Lu et al., 2017; Li et al., 2023b), yet raise privacy concerns due to the usage of personalized datasets. An alternative is running LLMs on user devices, but this is often impractical due to limited resource offered by the edge devices. Previous studies have introduced a range of algorithmic approaches to alleviate computational complexity (Zaken et al., 2021b; Guo et al., 2020b; Li and Liang, 2021; Wang et al., 2023; Lester et al., 2021; Mao et al., 2021b; He et al., 2021b; Liu et al., 2022; Deng, 2023; Peng et al., 2023b,a; Zhang, 2022; Zhang et al., 2023c) or enhance system performance (Jeong et al., 2018; Sheng et al., 2023; Lu et al., 2017; Li et al., 2023b,a). However, implementing these methods on edge devices is currently cost-prohibitive. This paper introduces DLoRA, a novel cloud-edge distributed system that offloads PEFT operations to edge devices, reducing computational and communication burdens while preserving privacy.

2.4 Federated Learning

Federated Learning (FL) (McMahan et al., 2017) has emerged as a groundbreaking approach to machine learning, enabling the creation of powerful

models by leveraging decentralized data sources while respecting user privacy. In contrast to FL, which conducts model training exclusively within edge devices, DLoRA introduces a collaborative distributed training framework between a single edge device with cloud servers. Additionally, DLoRA can also integrate with FL, facilitating fine-tuning processes across multiple edge devices.

3 Kill and Revive Mechanism

In this section, we describe *Kill and Revive* (KR) algorithm in detail, which aims to minimizing both computational and communication burdens on user devices during PEFT computations. We will begin by discussing the *Early-Kill* mechanism in Section 3.2, which is a simple yet effective approach to search for a minimal set of tunable parameters and eliminate redundant finetuning operations with negligible impact on accuracy. Following that, we will introduce the parameter revival mechanism in Section 3.3, which selects and reactivates a subset of previously frozen parameters, further enhancing the LLM accuracy.

3.1 Computation Pattern for DLoRA

To begin with, we first illustrate the computational pattern for a single round of DLoRA operation. As depicted in Figure 4, this procedure can be divided into two phases: forward propagation and backward propagation, which are highlighted in grey and blue in Figure 4, respectively. Initially, the user data is first processed by the embedding layer, with the outputs of the embedding layer sent to the cloud for forward propagation across rest layers. This approach inherently mitigates privacy risks by keeping user data local during the PEFT operation, with only the text embeddings being transmitted to the cloud server for subsequent processing. While recent research attempts have been made to reverse text embeddings to retrieve the original text (Pan et al., 2020; Morris et al., 2023), these efforts predominantly operate under the assumption that attackers have unlimited access to query the text embeddings model. However, in our scenario, this assumption is unrealistic because the text embedding model is implemented within user devices, and will deny all the external query attempts. Subsequently, the results from the frozen LLM blocks are sent back to the user devices for forward propagation across the PEFT modules, whose weights are stored on the user devices. This process continues until

Algorithm 1 KR Algorithm (simplified version)

- 1: **Inputs:** LLM module pool F ; Total number of layer L ; Selection criteria ϵ . Total finetuning epoch E ;
 - 2: \triangleright Pre-tuning phase
 - 3: Tune all PEFT modules within F for several iterations to collect statistics.
 - 4: Record the changes on l_2 norms for each module, define the selection criteria.
 - 5: \triangleright Main tuning phase
 - 6: **for** $0 \leq e \leq E - 1$ **do**
 - 7: **for** $l \in L$ **do**
 - 8: **if** l_2 norm change on l -th PEFT module less than ϵ **then**
 - 9: Frozen the PEFT module at layer l .
 - 10: **else**
 - 11: Activate l -th PEFT module.
 - 12: Finetune all active PEFT modules.
 - 13: Recalculate ϵ .
-

the final LLM output is generated. Consequently, the computation and communication overhead on user devices scales proportionally with the number of PEFT modules.

Likewise, the backward propagation begins with comparing the LLM output with the ground truth output, which further producing the gradient for the last LLM layer. These gradients are subsequently employed to compute output gradients for earlier layers, progressing until a PEFT module is reached. The gradients are then transmitted back to the user device for backward propagation and weight updates. This process continues until all the weights within the PEFT module have been updated. Likewise, as in the forward propagation scenario, the computational and communication overhead during backward propagation also scales in proportion to the number of PEFT modules.

3.2 Early Kill Mechanism

Considering the computation pattern outlined in Section 3.1, an simple strategy for reducing training cost over the user device is to simply reduce the amount of the PEFT modules. To achieve this while preserving the accuracy, DLoRA dynamically identifies the most relevant and significant PEFT modules that contribute most to downstream task accuracy, and only finetune these modules. To investigate the significance of PEFT modules towards training accuracy, we conduct experiments to evaluate the importance of each PEFT module

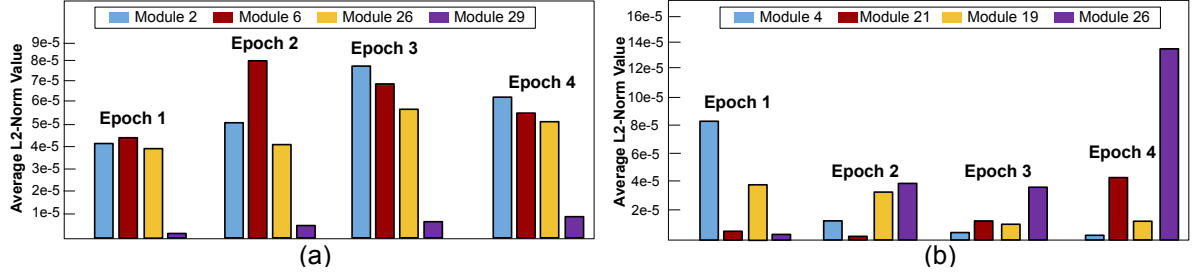


Figure 3: l_2 -norm variation of selected PEFT modules across training iterations over multiple downstream tasks including (a) Arc-Challenge, (b) Social-QA.

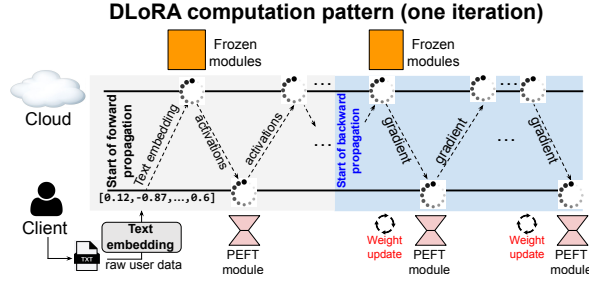


Figure 4: DLoRA computation pattern for one iteration.

using multiple training datasets. Specifically, we configure the PEFT module pool to comprise all the learnable parameters outlined in LoRA (Section 2.2), and make all the PEFT modules in the pool learnable. We then record the weights changes for different PEFT modules during the finetuning process. Figure 3 presents the variation on PEFT module magnitudes during the PEFT process over two downstream tasks. We notice a great variation on the PEFT module magnitudes across the finetuning iterations. For instance, in Figure 3 (a), PEFT module 6 (highlighted in red) exhibits an l_2 -Norm value exceeding $16\times$ the average l_2 -norm. This observation suggests that the parameters within this module undergo substantial changes during the PEFT process. We refer to the PEFT modules with substantial changes as *active PEFT modules*. On the contrary, PEFT module 29 (marked as purple) in Figure 3 (a) has a low l_2 norm value through the whole tuning process, which shows it exhibits no noticeable changes. We refer to blocks like that as *idle PEFT modules*. The Early Kill (EK) mechanism is designed to dynamically detect and freeze the idle PEFT modules to reduce computation and communication load on user devices. The EK mechanism comprises two phases, which are explained in detail below:

Pre-tuning Phase: In this phase, all the PEFT modules within the PEFT module pool are configured to be learnable. A short preliminary fine-

tuning is performed and the changes on the weight magnitudes for each PEFT modules are recorded. This change naturally reflects the degree of activities of each PEFT module.

Main tuning phase: We rank all the PEFT modules base on the magnitude differences recorded during the Pre-tuning phase. PEFT modules with magnitude change smaller than a predefined threshold are identified as idle PEFT module, which are then frozen (‘killed’) to enhance compute efficiency of user device.

3.3 Parameter Revival Mechanism

The EK technique, detailed in Section 3.2, enables us to selectively update only the active PEFT modules, resulting in substantial reductions in computation and communication for user devices. However, our evaluation results indicate a noticeable LLM accuracy drop when EK mechanism is applied. To better understand the reason, we analyze the magnitude variation across all the PEFT modules in LLaMA-7B model (Touvron et al., 2023) over social-qa (Sap et al., 2019) dataset. As depicted in Figure 3 (b), the PEFT module 26 (marked as purple) changes greatly in the 4th epoch while its parameters stay steady in the first three epochs. The PEFT module 4 (marked as blue) changes greatly in the first epoch and becomes stable after that. This phenomenon indicates that the active PEFT modules in the previous epoch may no longer be active in the later epochs, while the idle PEFT modules can become active in the later epochs.

The fluctuations in the weight magnitude presented in Figure 3 (b) indicate the need for regularly reviving the PEFT modules that were killed previously, as they could have a significant impact on LLM accuracy in the later stage of finetuning process. Based on this observation, we propose a *Kill and Revival (KR) Algorithm* (Algorithm 1). Specifically, at the end of each epoch of fine-tuning,

we rank all PEFT modules according to their magnitude changes within the epoch and kill the idle PEFT modules (Line 9 in Algorithm 1). In addition, we also pick a subset of killed PEFT modules and reactivate them (described in algorithm 1 line 13). The selection criteria for PEFT modules revival are determined by their l_2 norm changes during the last epoch in which they were active. The full version of algorithm 1 is in the Appendix section. While alternative criteria are feasible, we have noticed that employing the l_2 distance in the KR algorithm produces outstanding performance. To restrict the computation cost, we maintain a constant number of active PEFT modules across the entire finetuning process. By adhering to this *computation budget*, we ensure that the computation and communication costs of the user device remain consistent throughout the PEFT operation.

4 Evaluation

In this section, we provide a comprehensive evaluation of the KR algorithm and DLoRA System. We begin by describing the evaluation setup in Section 4.1. Next, we assess the accuracy and system performance of the KR algorithm across multiple tasks and LLMs in Section 4.2. Subsequently, we perform multiple ablation studies in Section 4.3.

4.1 Experiment Setup

Datasets and models: We evaluate our KR algorithm on three popular LLMs, including OPT-6.7B (Zhang et al., 2022), BLOOM-7B (Scao et al., 2022), and LLaMA-7B (Touvron et al., 2023). Additionally, we conduct evaluations of the KR algorithm across a range of tasks, including Question and Answering tasks such as OpenBookQA (OBQA) (Mihaylov et al., 2018), PIQA (Bisk et al., 2020), Social IQa (SIQA) (Sap et al., 2019) and BoolQ (Clark, 2019), problem compilation and concluding tasks including Winograde (ai2, 2019) and HellaSwag (Zellers et al., 2019) and multi-choice science questions such as ARC-easy and ARC-challenge (Clark et al., 2018).

PEFT Settings: In our study, experiments were conducted using the library from HUGGINGFACE (Huggingface, 2016). The AdamW (Pytorch, 2023) optimizer is employed in conjunction with a cosine learning rate scheduler throughout the training and fine-tuning processes. The accuracy evaluation for the KR algorithm are performed on an Nvidia A100-SMX4 platform (NVIDIA, 2021)

with 40GB memory. The software framework employed was CUDA, version 11.6. We conduct fine-tuning for a total of five epochs across all the downstream tasks. During the PEFT training, we always keep $B = 16$ PEFT modules to be active, so the computation budget B in Algorithm 2 is set to 16. Furthermore, we operate under the assumption that all intermediate results are in floating-point precision. We will explore the effects of quantizing the intermediate results in the Appendix.

DLoRA System Configuration: To measure the system performance of DLoRA in a practical environment, we have built a testbed with an Nvidia Jetson Xavier (NVIDIA, 2022) device and a cloud server to simulate the cloud and edge environment. We then measure the processing latency of the DLoRA system across various tasks. Details of hardware settings can be found in the Appendix.

Baselines: To fairly evaluate the accuracy performance of the KR algorithm, we compare it with a baseline algorithm termed Fully-tune (FT) algorithm, which keeps all the PEFT modules active throughout the entire finetuning process. In comparison, KR algorithm applies the Early kill mechanism described in Section 3.2 with the parameter-revival mechanism discussed in Section 3.3. The purpose of this baseline is to evaluate the importance of the parameter revival mechanism over the accuracy performance. For KR algorithm, we configure PEFT module pool to include all the LoRA parameters. To be noted here, our question-answering experiments are without any promotion, and we selected 25% of the dataset as training sets and left the rest 75% as testing sets. Due to the space limit, we include more evaluation results in the Appendix.

4.2 Evaluation Results

Table 1 displays the accuracy results for FT and KR across different LLMs and datasets. It is evident that KR achieves similar or even better performance compared to FT in a variety of tasks. For example, in task SIQA, KR obtains higher accuracies over FT all the LLMs. For the other datasets, we observe that KR can achieve a comparable performance with the FT algorithm, with significant reduction on compute and communication workload, which is detailed in Figure 5. The findings indicate that KR demonstrates better training efficiency compared to FT, achieving an average reduction of 82% in compute costs for user device operations.

LLM	Methods	BoolQ	PIQA	SIQA	WinoGrande	OBQA	ARC-easy	ARC-challenge
BloomZ	FT	64.6%	71.0%	75.4%	60.8%	72.2%	75.4%	45.9%
	DLoRA	64.6% (+0.0%)↑	73.7% (+2.7%)↑	73.2% (+2.2%)↑	65.0% (+4.2%)↑	72.1% (-0.1%)↓	75.1% (-0.3%)↓	44.6% (-1.3%)↓
LLaMA-7B	FT	70.7%	80.9%	75.6%	66.5%	70.0%	65.5%	47.9%
	DLoRA	74.3% (+3.6%)↑	79.7% (-1.2%)↓	77.0% (+1.4%)↑	65.7% (-1.8%)↓	73.8% (+3.8%)↑	71.6% (+6.1%)↑	46.7% (-1.2%)↓
OPT	FT	66.6%	74.4%	72.2%	50.4%	33.8%	46.0%	26.2%
	DLoRA	64.8% (-1.2%)↓	78.0% (+3.6%)↑	72.6% (+0.4%)↑	48.0% (-2.4%)↓	35.4% (+1.6%)↑	46.0% (+0.0%)↑	28.8% (+2.6%)↑

Table 1: Accuracy performance evaluation of FT and DLoRA across all the tasks over different LLMs. The changes on accuracies are also highlighted in green or red.

LLM	Budgets	BoolQ	PIQA	SIQA	HellaSwag	WinoGrande	OBQA	ARC-easy	ARC-challenge
Bloom-Z	16 (baseline)	64.6%	70.5%	73.2%	67.5%	65.0%	72.1%	75.1%	44.6%
	8	+7.7%↑	+4.3%↑	+0.8%↑	-4.5%↓	-1.4%↓	-3.3%↓	-1.5%↓	-6.2%↓
	4	-8.2%↓	+3.7%↑	-4.6%↓	-3.7%↓	+8.0%↑	+0.9%↑	-0.1%↓	-3.8%↓
LLaMA	16 (baseline)	74.3%	79.7%	77.0%	73.6%	65.7%	73.8%	71.6%	46.7%
	8	-6.0%↓	-0.4%↓	+1.1%↑	+2.5%↑	+5.6%↑	-2.6%↓	-6.0%↓	+0.5%↑
	4	-8.2%↓	+0.0%	+1.7%↑	+3.8%↑	-6.4%↓	-3.8%↓	-0.6%↓	+0.5%↑
OPT	16 (baseline)	64.8%	78.0%	72.6%	45.0%	48.0%	35.4%	46.0%	28.8%
	8	-1.6%↓	-2.0%↓	+0.0%	+0.6%↑	+3.6%↑	-1.4%↓	-0.8%↓	+1.0%↑
	4	-3.0%↓	-1.6%↓	-5.4%↓	-0.4%↓	+1.4%↑	-3.4%↓	-2.4%↓	-0.8%↓

Table 2: Accuracy performance under different compute budget. For each dataset, we use the accuracy of KR with a compute budget of 16 as the baseline and describe the changes in accuracy relative to it.

Dataset/Method	DLoRA	SparseGPT	Wanda
PIQA	79.7%	73.1%	73.0%
HellaSwag	73.6%	44.8%	43.6%
OBQA	73.8%	62.6%	63.6%
ARC-E	71.6%	30.2%	30.3%
ARC-C	46.7%	24.4%	25.0%
# learnable param.	1.1M	10.41B	10.69B
Peak memory cost	4.2MB	38.74GB	39.82 GB

Table 3: Accuracy performance and learnable parameters compared to different LLM pruning mechanisms. DLoRA outperforms SparseGPT and Wanda in terms of both accuracy and peak memory utilization.

Additionally, similar computational savings are observed when applying KR algorithm with Adapter scheme. This is attributed to the fact that the KR algorithm dynamically selects and maintains a minimal set of active modules for execution within the user device, resulting in a notable reduction in computational load. For additional evaluations, please refer to the Appendix section.

Finally, Figure 5 shows the total amount of communication during one epoch of the PEFT process for FT and KR across various tasks. In contrast to FT, KR attains an average reduction of 87.5% in communication, underscoring the efficiency of the KR algorithm in terms of communication. In summary, we conclude that the KR algorithm is capable

of achieving significant reductions in both computation and communication, all the while maintaining comparable levels of accuracy to FT.

4.3 Ablation Studies

Impact on computation budget To better understand the impact of computation budget over the accuracy performance, we change the computation budget B from 16 to 8 and 4, and evaluate the accuracy performance. As shown in Table 2, there is a general trend of accuracy degradation as the computation budget decreases, primarily due to the reduction in the number of learnable parameters in the LLM. Interestingly, accuracy improves for certain tasks even when computation budgets are reduced. For example, when training Bloom-Z with the PIQA and Boolq datasets, it outperforms the performance of KR with a computation budget of 16. This suggests that only a smaller subset of PEFT modules are responsive to the downstream tasks specified by the Bloom-Z dataset.

Comparison With LLM compression In addition to FT, we explore an alternative baseline algorithm that applies pruning techniques to reduce the size of backbone models. This strategy enhances computational efficiency for PEFT operations, making the PEFT process implementable on edge devices. Specifically, we evaluate two recent methods, SparseGPT (Frantar and Alistarh,

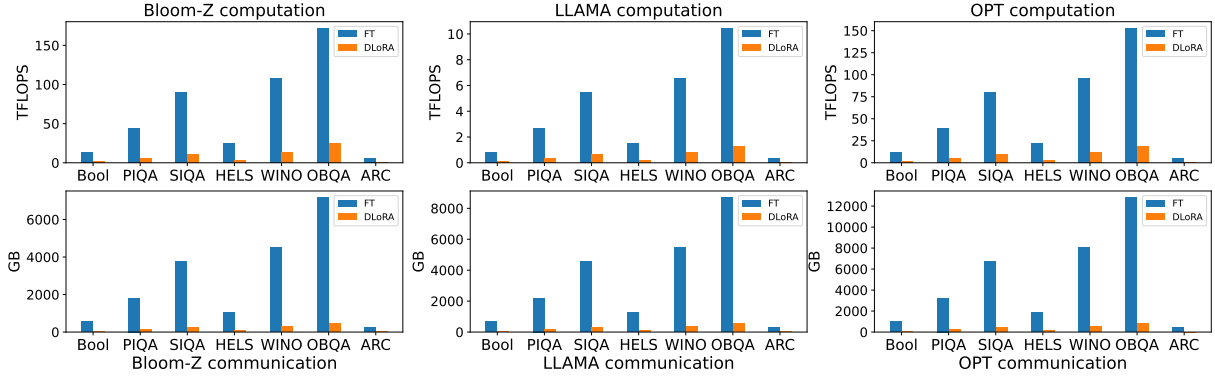


Figure 5: Computation costs of KR and FT over different LLMs, the measurement denotes the computation cost in TFLOPs. The communication costs for KR and FT are measured in Gigabytes (GB).

2023) and Wanda (Sun et al., 2023). SparseGPT and Wanda propose efficient Post-Training-Pruning mechanisms to reduce the number of parameters on LLM models, each of them proposes innovative selection criteria for pruning operation, optimizing the sparse LLM accuracy. We evaluate Wanda and SparseGPT with zero-shot prompting on a single A100 GPU. Table 3 indicates that DLoRA outperforms SparseGPT and Wanda in terms of both accuracy performance and peak memory usage. Additionally, DLoRA also incurs much smaller computational cost.

System Latency Measurement Next, we measure the processing latency required to complete one epoch of PEFT for DLoRA over the real edge device. The detail system settings are described in Section 6.3 of Appendix. The measurement reveals that with LoRA finetuned using FT, a single epoch of PEFT over Bloom-Z on OpenbookQA will consume 200.72s. This latency includes the processing time on both the cloud server and the user device. In contrast, with the DLoRA, a single epoch of PEFT only takes 182.59 seconds. This is attributed to the fact that DLoRA greatly reduces the computational workload on the user device, resulting in a decrease in overall processing latency. Table 3 shows that our DLoRA system outperforms other baseline algorithms in both accuracy and peak memory usage.

DLoRA on Adapter We evaluate DLoRA performance with Serial Adapter (Hu et al., 2023) over different downstream tasks and LLMs. All the settings are kept the same as those described in Section 4.1. The evaluation on accuracies are presented in Table 4. We notice that DLoRA also outperforms FT over multiple tasks and LLMs, demonstrating

LLM	Methods	BoolQ	PIQA	OBQA	ARC-challenge
BloomZ	FT	66.0%	78.2%	65.4%	44.2%
	DLoRA	70.0% (+3.4%) [†]	76.2% (-2.0%)	72.0% (+6.6%)	45.8% (+1.6%)
LLaMA-7B	FT	63.7%	71.0%	70.0%	45.3%
	DLoRA	67.2% (+3.5%) [†]	79.4% (+8.4%) [†]	73.1% (+3.1%) [†]	44.0% (-1.3%) [‡]
OPT	FT	62.8%	76.8%	41.0%	26.0%
	DLoRA	67.4% (+4.6%) [†]	79.4% (+2.6%) [†]	43.8% (+2.8%) [†]	26.0% (+0.0%) [†]

Table 4: Accuracy performance evaluation with Adapter across all the tasks over different LLMs.

the generalizability of DLoRA across various fine-tuning schemes.

Impact of Quantization Precision By default, the activation and gradient matrices exchanged between the cloud and the user device are encoded as a 32-bit floating-point number. To further reduce communication costs, we implement low-precision quantization on the transmitted data, mapping the original full-precision numbers to their nearest quantized values. To demonstrate the impact of quantization precision, we employ 8-bit precision to quantize all communication between the cloud and the user device during the PEFT, compared with floating-point precision, this will further lead to 4× saving on communication overhead. The results across various datasets under different computer budgets are presented in Table 5. It is observed that the accuracies experience a modest decrease. More quantization results are presented in Appendix.

5 Conclusion

The paper introduces DLoRA, a novel distributed solution tailored for efficient PEFT operations spanning cloud and edge devices. DLoRA utilizes the Kill and Revive algorithm to enhance efficiency during the fine-tuning process, resulting in substantial reductions in computational and communica-

LLM	Compute Budget	BoolQ	PIQA	SIQA
Bloom-Z	Baseline	64.6%	70.5%	73.2%
	Q=8, B=16	+1.8%↑	+5.1%↑	+1.6%↑
	Q=8, B=8	+1.6%↑	+4.6%↑	-0.6%↓
	Q=8, B=4	+0.2%↑	+3.6%↑	-1.8%↓

Table 5: Accuracies under different budget (B) and quantization bitwidth (Q). We present the accuracy variations relative to the baseline setting (B=16, Q=32).

tion workloads. Experimental findings illustrate that compared to both cloud-only and edge-only solutions, our DLoRA system notably minimizes computation and communication while upholding accuracy and privacy.

References

2019. Winogrande: An adversarial winograd schema challenge at scale.
- Mariam Badr. 2023. Unleashing the power of ai: the microsoft and openai partnership.
- Yonatan Bisk, Rowan Zellers, Ronan Le Bras, Jianfeng Gao, and Yejin Choi. 2020. Piqa: Reasoning about physical commonsense in natural language. In *Thirty-Fourth AAAI Conference on Artificial Intelligence*.
- Tom Brown, Benjamin Mann, Nick Ryder, Melanie Subbiah, Jared D Kaplan, Prafulla Dhariwal, Arvind Neelakantan, Pranav Shyam, Girish Sastry, Amanda Askell, et al. 2020. Language models are few-shot learners. *Advances in neural information processing systems*, 33:1877–1901.
- Christopher et al. Clark. 2019. Boolq: Exploring the surprising difficulty of natural yes/no questions. In *NAACL*.
- Peter Clark, Isaac Cowhey, Oren Etzioni, Tushar Khot, Ashish Sabharwal, Carissa Schoenick, and Oyvind Tafjord. 2018. Think you have solved question answering? try arc, the ai2 reasoning challenge. *arXiv:1803.05457v1*.
- Yiming Cui, Ziqing Yang, and Xin Yao. 2023. Efficient and effective text encoding for chinese llama and alpaca. *arXiv preprint arXiv:2304.08177*.
- et al Deng, Mingkai. 2023. Rlprompt: Optimizing discrete text prompts with reinforcement learning. <https://arxiv.org/pdf/2205.12548>.
- Elias Frantar and Dan Alistarh. 2023. Sparsegpt: Massive language models can be accurately pruned in one-shot. In *International Conference on Machine Learning*, pages 10323–10337. PMLR.
- Peng Gao, Jiaming Han, Renrui Zhang, Ziyi Lin, Shijie Geng, Aojun Zhou, Wei Zhang, Pan Lu, Conghui He, Xiangyu Yue, et al. 2023. Llama-adapter v2: Parameter-efficient visual instruction model. *arXiv preprint arXiv:2304.15010*.
- Demi Guo, Alexander M Rush, and Yoon Kim. 2020a. Parameter-efficient transfer learning with diff pruning. *arXiv preprint arXiv:2012.07463*.
- Demi Guo, Alexander M Rush, and Yoon Kim. 2020b. Parameter-efficient transfer learning with diff pruning. *arXiv preprint arXiv:2012.07463*.
- Muhammad Usman Hadi, R Qureshi, A Shah, M Irfan, A Zafar, MB Shaikh, N Akhtar, J Wu, and S Mirjalili. 2023. A survey on large language models: Applications, challenges, limitations, and practical usage. *TechRxiv*.
- Junxian He, Chunting Zhou, Xuezhe Ma, Taylor Berg-Kirkpatrick, and Graham Neubig. 2021a. Towards a unified view of parameter-efficient transfer learning. *arXiv preprint arXiv:2110.04366*.

- Junxian He, Chunting Zhou, Xuezhe Ma, Taylor Berg-Kirkpatrick, and Graham Neubig. 2021b. Towards a unified view of parameter-efficient transfer learning. *arXiv preprint arXiv:2110.04366*.
- Shwai He, Liang Ding, Daize Dong, Jeremy Zhang, and Dacheng Tao. 2022. [SparseAdapter: An easy approach for improving the parameter-efficiency of adapters](#). In *Findings of the Association for Computational Linguistics: EMNLP 2022*, pages 2184–2190, Abu Dhabi, United Arab Emirates. Association for Computational Linguistics.
- Neil Houlsby, Andrei Giurgiu, Stanislaw Jastrzebski, Bruna Morrone, Quentin De Laroussilhe, Andrea Gesmundo, Mona Attariyan, and Sylvain Gelly. 2019. Parameter-efficient transfer learning for nlp. In *International Conference on Machine Learning*, pages 2790–2799. PMLR.
- Edward J Hu, Yelong Shen, Phillip Wallis, Zeyuan Allen-Zhu, Yanzhi Li, Shean Wang, Lu Wang, and Weizhu Chen. 2021. Lora: Low-rank adaptation of large language models. *arXiv preprint arXiv:2106.09685*.
- Zhiqiang Hu, Yihuai Lan, Lei Wang, Wanyu Xu, Ee-Peng Lim, Roy Ka-Wei Lee, Lidong Bing, and Soujanya Poria. 2023. Llm-adapters: An adapter family for parameter-efficient fine-tuning of large language models. *arXiv preprint arXiv:2304.01933*.
- Huggingface. 2016. Hugging face. In <https://huggingface.co/>.
- Hyuk-Jin Jeong, Hyeon-Jae Lee, Chang Hyun Shin, and Soo-Mook Moon. 2018. Ionn: Incremental offloading of neural network computations from mobile devices to edge servers. In *Proceedings of the ACM symposium on cloud computing*, pages 401–411.
- Rabeeh Karimi Mahabadi, James Henderson, and Sebastian Ruder. 2021a. Compacter: Efficient low-rank hypercomplex adapter layers. *Advances in Neural Information Processing Systems*, 34:1022–1035.
- Rabeeh Karimi Mahabadi, James Henderson, and Sebastian Ruder. 2021b. Compacter: Efficient low-rank hypercomplex adapter layers. *Advances in Neural Information Processing Systems*, 34:1022–1035.
- Brian Lester, Rami Al-Rfou, and Noah Constant. 2021. The power of scale for parameter-efficient prompt tuning. *arXiv preprint arXiv:2104.08691*.
- Xiang Lisa Li and Percy Liang. 2021. Prefix-tuning: Optimizing continuous prompts for generation. *arXiv preprint arXiv:2101.00190*.
- Zexin Li, Tao Ren, Xiaoxi He, and Cong Liu. 2023a. [Red: A systematic real-time scheduling approach for robotic environmental dynamics](#). In *2023 IEEE Real-Time Systems Symposium (RTSS)*, pages 210–223.
- Zexin Li, Aritra Samanta, Yufei Li, Andrea Soltoggio, Hyoseung Kim, and Cong Liu. 2023b. R^3 : On-device real-time deep reinforcement learning for autonomous robotics. *arXiv preprint arXiv:2308.15039*.
- Haokun Liu, Derek Tam, Mohammed Muqeeth, Jay Mohhta, Tenghao Huang, Mohit Bansal, and Colin A Raffel. 2022. Few-shot parameter-efficient fine-tuning is better and cheaper than in-context learning. *Advances in Neural Information Processing Systems*, 35:1950–1965.
- Wenyan Lu, Guihai Yan, Jiajun Li, Shijun Gong, Yinhe Han, and Xiaowei Li. 2017. [Flexflow: A flexible dataflow accelerator architecture for convolutional neural networks](#). In *2017 IEEE International Symposium on High Performance Computer Architecture (HPCA)*, pages 553–564.
- Yuning Mao, Lambert Mathias, Rui Hou, Amjad Almahairi, Hao Ma, Jiawei Han, Wen-tau Yih, and Madian Khabsa. 2021a. Unipelt: A unified framework for parameter-efficient language model tuning. *arXiv preprint arXiv:2110.07577*.
- Yuning Mao, Lambert Mathias, Rui Hou, Amjad Almahairi, Hao Ma, Jiawei Han, Wen-tau Yih, and Madian Khabsa. 2021b. Unipelt: A unified framework for parameter-efficient language model tuning. *arXiv preprint arXiv:2110.07577*.
- Brendan McMahan, Eider Moore, Daniel Ramage, Seth Hampson, and Blaise Agüera y Arcas. 2017. Communication-efficient learning of deep networks from decentralized data. In *Artificial intelligence and statistics*, pages 1273–1282. PMLR.
- Todor Mihaylov, Peter Clark, Tushar Khot, and Ashish Sabharwal. 2018. Can a suit of armor conduct electricity? a new dataset for open book question answering. In *EMNLP*.
- John X Morris, Volodymyr Kuleshov, Vitaly Shmatikov, and Alexander M Rush. 2023. Text embeddings reveal (almost) as much as text. *arXiv preprint arXiv:2310.06816*.
- NVIDIA. 2021. Nvidia a100 tensor core gpu. <https://www.nvidia.com/en-us/data-center/a100/>.
- NVIDIA. 2022. Nvidia jetson xavier. <https://www.nvidia.com/en-us/autonomous-machines/embedded-systems/jetson-xavier-series/>.
- OpenAI and Microsoft. 2023. <https://openai.com/blog/openai-and-microsoft>.
- Xudong Pan, Mi Zhang, Shouling Ji, and Min Yang. 2020. Privacy risks of general-purpose language models. In *2020 IEEE Symposium on Security and Privacy (SP)*, pages 1314–1331. IEEE.
- Hongwu Peng, Shaoyi Huang, Tong Zhou, Yukui Luo, Chenghong Wang, Zigeng Wang, Jiahui Zhao, Xi Xie,

- Ang Li, Tony Geng, et al. 2023a. Autorep: Automatic relu replacement for fast private network inference. In *Proceedings of the IEEE/CVF International Conference on Computer Vision*, pages 5178–5188.
- Hongwu Peng, Shanglin Zhou, Yukui Luo, Nuo Xu, Shijin Duan, Ran Ran, Jiahui Zhao, Shaoyi Huang, Xi Xie, Chenghong Wang, et al. 2023b. Rnet: Towards relu-reduced neural network for two-party computation based private inference. *arXiv preprint arXiv:2302.02292*.
- Jonas Pfeiffer, Ivan Vulić, Iryna Gurevych, and Sebastian Ruder. 2020. Mad-x: An adapter-based framework for multi-task cross-lingual transfer. *arXiv preprint arXiv:2005.00052*.
- Pytorch. 2023. Adamw optimizer. In <https://pytorch.org>.
- Baptiste Roziere, Jonas Gehring, Fabian Gloeckle, Sten Sootla, Itai Gat, Xiaoqing Ellen Tan, Yossi Adi, Jingyu Liu, Tal Remez, Jérémy Rapin, et al. 2023. Code llama: Open foundation models for code. *arXiv preprint arXiv:2308.12950*.
- Andreas Rücklé, Gregor Geigle, Max Glockner, Tilman Beck, Jonas Pfeiffer, Nils Reimers, and Iryna Gurevych. 2020. Adapterdrop: On the efficiency of adapters in transformers. *arXiv preprint arXiv:2010.11918*.
- Maarten Sap, Hannah Rashkin, Derek Chen, Ronan LeBras, and Yejin Choi. 2019. Socialliqa: Commonsense reasoning about social interactions. *arXiv preprint arXiv:1904.09728*.
- Teven Le Scao, Angela Fan, Christopher Akiki, Ellie Pavlick, Suzana Ilić, Daniel Hesslow, Roman Castagné, Alexandra Sasha Luccioni, François Yvon, Matthias Gallé, et al. 2022. Bloom: A 176b-parameter open-access multilingual language model. *arXiv preprint arXiv:2211.05100*.
- Ying Sheng, Lianmin Zheng, Binhang Yuan, Zhuohan Li, Max Ryabinin, Beidi Chen, Percy Liang, Christopher Re, Ion Stoica, and Ce Zhang. 2023. Flexgen: High-throughput generative inference of large language models with a single gpu.
- Mingjie Sun, Zhuang Liu, Anna Bair, and J Zico Kolter. 2023. A simple and effective pruning approach for large language models. *arXiv preprint arXiv:2306.11695*.
- Hugo Touvron, Thibaut Lavril, Gautier Izacard, Xavier Martinet, Marie-Anne Lachaux, Timothée Lacroix, Baptiste Rozière, Naman Goyal, Eric Hambro, Faisal Azhar, et al. 2023. Llama: Open and efficient foundation language models. *arXiv preprint arXiv:2302.13971*.
- Mojtaba Valipour, Mehdi Rezagholizadeh, Ivan Kobzyev, and Ali Ghodsi. 2022. Dylora: Parameter efficient tuning of pre-trained models using dynamic search-free low-rank adaptation. *arXiv preprint arXiv:2210.07558*.
- Sid Wang, John Nguyen, Ke Li, and Carole-Jean Wu. 2023. Read: Recurrent adaptation of large transformers. *arXiv preprint arXiv:2305.15348*.
- Yaqing Wang, Subhabrata Mukherjee, Xiaodong Liu, Jing Gao, Ahmed Hassan Awadallah, and Jianfeng Gao. 2022. Adamix: Mixture-of-adapter for parameter-efficient tuning of large language models. *arXiv preprint arXiv:2205.12410*, 1(2):4.
- Elad Ben Zaken, Shauli Ravfogel, and Yoav Goldberg. 2021a. Bitfit: Simple parameter-efficient fine-tuning for transformer-based masked language-models. *arXiv preprint arXiv:2106.10199*.
- Elad Ben Zaken, Shauli Ravfogel, and Yoav Goldberg. 2021b. Bitfit: Simple parameter-efficient fine-tuning for transformer-based masked language-models. *arXiv preprint arXiv:2106.10199*.
- Rowan Zellers, Ari Holtzman, Yonatan Bisk, Ali Farhadi, and Yejin Choi. 2019. Hellaswag: Can a machine really finish your sentence? In *Proceedings of the 57th Annual Meeting of the Association for Computational Linguistics*.
- Hang Zhang, Xin Li, and Lidong Bing. 2023a. Video-llama: An instruction-tuned audio-visual language model for video understanding. *arXiv preprint arXiv:2306.02858*.
- Haopeng Zhang, Xiao Liu, and Jiawei Zhang. 2023b. Summit: Iterative text summarization via chatgpt. *arXiv preprint arXiv:2305.14835*.
- Jingyao Zhang, Mohsen Imani, and Elaheh Sadredini. 2023c. Bp-ntt: Fast and compact in-sram number theoretic transform with bit-parallel modular multiplication. In *2023 60th ACM/IEEE Design Automation Conference (DAC)*, pages 1–6.
- Jingyao et al Zhang. 2022. Inhale: Enabling high-performance and energy-efficient in-sram cryptographic hash for iot. In *Proceedings of the 41st IEEE/ACM International Conference on Computer-Aided Design, ICCAD '22, New York, NY, USA*. Association for Computing Machinery.
- Renrui Zhang, Jiaming Han, Aojun Zhou, Xiangfei Hu, Shilin Yan, Pan Lu, Hongsheng Li, Peng Gao, and Yu Qiao. 2023d. Llama-adapter: Efficient fine-tuning of language models with zero-init attention. *arXiv preprint arXiv:2303.16199*.
- Susan Zhang, Stephen Roller, Naman Goyal, Mikel Artetxe, Moya Chen, Shuohui Chen, Christopher Dewan, Mona Diab, Xian Li, Xi Victoria Lin, et al. 2022. Opt: Open pre-trained transformer language models. *arXiv preprint arXiv:2205.01068*.
- Wenhao Zhu, Hongyi Liu, Qingxiu Dong, Jingjing Xu, Lingpeng Kong, Jiajun Chen, Lei Li, and Shujian Huang. 2023. Multilingual machine translation with large language models: Empirical results and analysis. *arXiv preprint arXiv:2304.04675*.

Yuchen Zhuang, Yue Yu, Kuan Wang, Haotian Sun, and Chao Zhang. 2023. Toolqa: A dataset for llm question answering with external tools. *arXiv preprint arXiv:2306.13304*.

6 Appendix

In the supplementary material, we begin by describing the experimental settings of the system (Section 6.1). We present the complete version of the KR algorithm in section 6.2. In section 6.3, we depict the DLoRA system.

6.1 Experiment Setup

Table 6 lists the hyperparameter we used for the KR algorithm. We adhere to the parameter configuration specified in the original papers for LoRA (Hu et al., 2021) and Adapter (Zhang et al., 2023d). And Table list the hardware settings for the DLoRA cloud environment and edge devices.

Hyper Parameters	
Training epoch	4
Warm-up epoch	1
Batch size	16
Learning rate	3e-4
LoRA embedding dimension (D_m)	8
Adapter embedding dimension	128
Optimizer	adamW

Table 6: KR algorithm settings.

6.2 KR algorithm illustration

The fluctuations in the weight magnitude presented in Figure 3 (b) indicate the need for regularly reviving the PEFT modules that were killed previously, as they could have a significant impact on LLM accuracy. Based on this observation, we propose a Kill and Revival Algorithm (Algorithm 2). Specifically, at the end of each epoch of fine-tuning, we rank all PEFT modules according to their magnitude changes within the epoch and kill the idle PEFT modules (Line 12 in Algorithm 2). In addition, we also pick a subset of killed PEFT modules and reactivate them (described in algorithm 2 line 14). The selection criteria for PEFT modules revival are determined by their L2-norm changes during the last epoch in which they were active. Lastly, we maintain a constant number of active PEFT modules across the entire finetuning process. By adhering to this computation budget, we ensure that the computation and communication costs of the user device remain consistent throughout the PEFT operation.

Algorithm 2 Kill and Revive Algorithm

```

1: Inputs: LLM module F; Total number of layer
   L; Total finetuning epoch E; Computation bud-
   get  $B$ ; List of L2-Norm value  $N = \{N_{i,j}\}$ ,
    $0 \leq i \leq 2E + 1$ ;  $0 \leq j \leq L - 1$ , List of L2-
   Norm changes  $D = \{D_{i,j}\}$ ,  $0 \leq i \leq E - 1$ ,
    $0 \leq j \leq L - 1$ ;
2:  $\triangleright$  Pre-tuning phase
3:  $N_{0,1 \leq l \leq L} = \text{L2-Norm}(F)$ 
4: Tune all PEFT modules within F for several
   iterations to collect statistics.
5:  $N_{1,1 \leq l \leq L} = \text{L2-Norm}(F)$ 
6:  $D_{0,1 \leq l \leq L} = \text{DIFF}(N_0, N_1)$ 
7:  $\triangleright$  Main tuning phase
8: for  $0 \leq e \leq E - 1$  do
9:   Sort and take the  $B$ -th smallest value from
    $D_e$ , denote as  $T$ .
10:  for  $l \in L$  do
11:    if  $D_{e,l} < T$  then
12:      Kill  $l$ -th PEFT module in F
13:    else
14:      Activate  $l$ -th PEFT module in F
15:     $N_{2e+2,1 \leq l \leq L} = \text{L2-Norm}(F)$ 
16:    Finetune all active PEFT modules by one
   epoch.
17:     $N_{2e+3,1 \leq l \leq L} = \text{L2-Norm}(F)$ 
18:     $D_{e+1,1 \leq l \leq L} = \text{DIFF}(N_{2e+2}, N_{2e+3})$ 
19:     $\triangleright$  Reviving Phase
20:    for  $l \in L$  do
21:      if  $D_{e+1,l} = 0$  then
22:         $D_{e+1,l} = D_{e,l}$ 
23:   $\triangleright$  Function to compute L2-Norm Value differ-
   ence
24:  function  $\text{DIFF}(A_1, A_2)$ 
25:    for  $1 \leq i \leq \text{length}(A_1)$  do
26:       $A_{1,i} = |A_{1,i} - A_{2,i}|/A_{1,i}$ 
27:    return  $A_1$ 
28:   $\triangleright$  Function to compute L2-Norm Value
29:  function  $\text{L2-NORM}(F)$ 
30:    Initialize Norm = []
31:    for every decoder block d in F do
32:      Append  $l_2$  norm of d to Norm.
33:    return Norm

```

LLM	Budgets	BoolQ	PIQA	SIQA	HellaSwag	WinoGrande	OBQA	ARC-easy	ARC-challenge
Bloom-Z	16 (baseline)	70.0%	76.2%	72.4%	68.0%	63.4%	72.0%	69.8%	45.8%
	8	-1.4%↓	+1.0%↑	0.0%	+4.0%↑	-1.2%↓	+1.0%↑	+1.8%↑	-3.3%↓
	4	-3.0%↓	+0.8%↑	-1.6%↓	+3.4%↑	-4.0%↓	-8.2%↓	-3.8%↓	-4.6%↓
LLaMA	16 (baseline)	66.4%	79.4%	72.4%	75.4%	73.1%	73.1%	63.6%	44.0%
	8	-0.7%↓	+1.2%↑	-6.0%↓	+5.6%↑	-1.7%↓	+1.3%↑	-1.1%↓	+6.6%↑
	4	-3.8%↓	+1.1%↑	-8.0%↓	-0.7%↓	-1.8%↓	+0.7%↑	-11.6%↓	+0.6%↑
OPT	16 (baseline)	67.74%	74.40%	72.20%	47.8%	50.4%	33.8%	46.0%	26.2%
	8	+4.4%↑	+5.2%↑	+0.4%↑	+1.6%↑	+2.6%↑	+8.8%↑	+3.4%↑	-3.2%↓
	4	+4.0%↑	+1.6%↑	+0.2%↑	+2.0%↑	+2.2%↑	+8.2%↑	+1.0%↑	-2.0%↓

Table 7: Accuracy performance under different compute budgets for the Adapter. For each dataset, we use the same setting as Table 2.

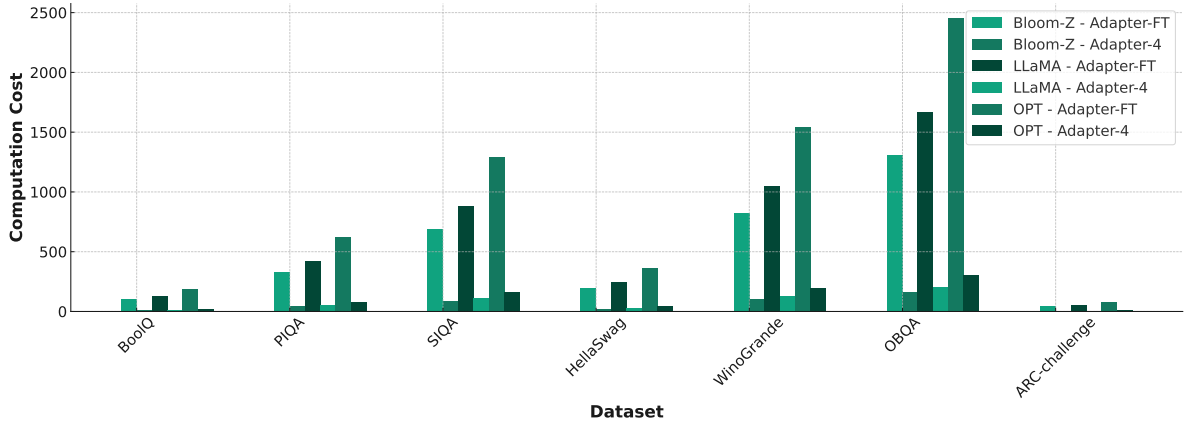


Figure 6: Computation costs of KR algorithms and full-fine tuning over different LLMs with Adapter, the measurement denotes the computation cost in TFLOPs.

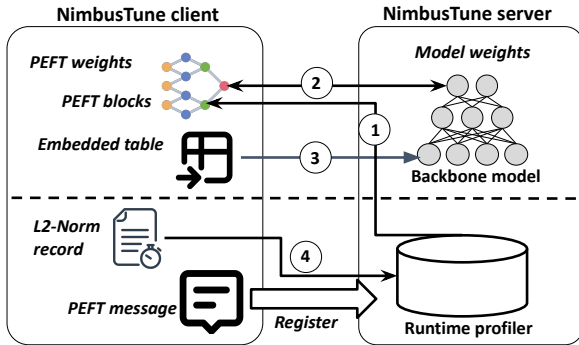


Figure 7: System architecture of DLoRA

6.3 System Overview

As depicted in Figure 7, DLoRA system comprises a cloud server and a user device. It is noteworthy that DLoRA can be easily scaled to accommodate additional user devices. The cloud server contains three major components: a compute engine, a system scheduler, and a message queue. The compute engine can support open-source Huggingface API (Huggingface, 2016) for LLM operation. The

pivotal component of the DLoRA system is the system scheduler, tasked with managing edge/cloud synchronization and distributing the kill and revival commands for efficient PEFT operations outlined in Section 3. The message queue functions as the communication tunnel between the central server and user device. The messages can be categorized into three types: 1. intermediate activation and gradient values generated during the PEFT computation; 2. l2 Norm of the PEFT module parameters at the end of each epoch for the KR algorithm execution; 3. Kill/Revival messages from the cloud server. Likewise, the user device is equipped with a compute engine and a message queue. The primary difference lies in the compute engine, which is dedicated to the lightweight fine-tuning of active PEFT modules and the computations related to embedding layers.